The research of the spectral characteristics of the voltage inverter exciter bandwidth

O Miroshnyk[1], R Lysychenko[1], S Kovalyshyn[2], W Kruszelnicka[3], P Bałdowska-Witos[3] and A Tomporowski[3]

[1]Kharkiv Petro Vasylenko National Technical University of Agriculture, Alchevskyh St, no. 44, 61002 Kharkiv, Ukraine
[2]Lviv National Agrarian University, Volodomyra Velyhoko St, no. 1, 30831 Dublyany, Ukraine
[3]University of Science and Technology in Bydgoszcz, Al. Prof. S. Kaliskiego, no. 7, 85-793 Bydgoszcz, Poland

E-mail: omiroshnyk@ukr.net

Abstract. The analysis of the structural scheme of the reflectometric system exciter was carried out. We show that the basic block diagram for the construction of range of the inverter is a single ring exciter digital frequency synthesizer. The mathematical model of range of the inverter exciter provides an analysis of the structural schemes of inverter with pathogen spectral methods. These expressions of the spectral power density of the phase fluctuations allowed to take into account the effect of the circuit elements of the inverter of the pathogen on its spectral characteristics and calculate the dispersion, the average deviation of the phase in the frequency band and the mean square raid exciter output signal phase.

1. Introduction

The trend of wide implementation of voltage inverters in various industries is forcing to focus on issues related to electromagnetic compatibility. For example, modern power inverters keys, especially MOSFET and IGBT with have very high switching speed, become sources of electromagnetic interference. The range of generated interference extends from the carrier frequency of the inverter (several hundreds of KHz) to radio frequency (tens of MHz). Low-frequency interferences up to 2 kHz penetrate into the supply network, high-frequency (> 10 kHz) components create a powerful radio interference [1-4].

The non-linear nature of the circuit, which determined by the existence of semiconductor elements (diodes, transistors, thyristors, etc.) which are part of the inverter structure chart, is the reason for generating the higher harmonics. Therefore, we carry out a research on the effects of the non-linear nature of the drivers elements, namely the research of influence of range exciters and inventers systems of phase timing on the spectral characteristics.

One of the major problems which must be solved during design and production of the voltage inverter is to eliminate adverse effect of the exciter on the technical characteristics (TC) of the inverter, in particular on electromagnetic compatibility. Thereby, the development of recommendations on the choice the optimal parameter values of the phase-locked loop (PLL) of frequency synthesizer on the basis of accurate numerical analysis occurring therein is very important.

It is known that the PLL is generally described by non-linear differential equations [5].

For the calculated ratios we used the Volterra functional expansion technique, which currently is one of the most convenient and accurate methods for analyzing non-linear dynamic systems [6, 7].

2. Experiment

As the main circuit of direct digital synthesizers (DDS) of range exciters (which basing on the analysis of modern element base we choose the single-ringed PLL circuit in the backward circuit which is placed a frequency divider with variable division ratio of the frequency divider with variable division factor (FDVD).
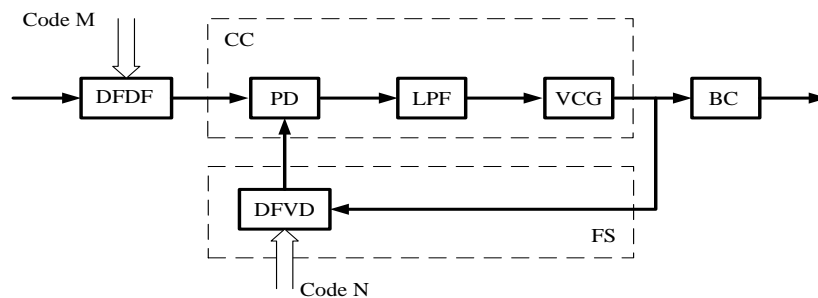
Figure 1. Synthesizer structure chart with the pulse-phase-locked loop (PPLL): FS – feedback section, BC – buffer cascade, VCG – voltage-controlled generator, DFVD – a frequency divider with variable division ratio, LPF – low-pass filter, PD – phase discriminator, CC – control channel, DFDF – a frequency divider with a fixed division factor

The loop consists of a voltage-controlled generator, a frequency divider with variable division ratio, phase discriminator and low-pass filter. The frequency of a voltage-controlled generator divides and compares with a stable reference frequency [8], [9]. The error voltage is produced with a phase discriminator and it is used to stabilize the frequency of a voltage-controlled generator. Output frequency setting is produced with a personal computer (PC) command or from a control panel which changes the distribution ratio of a frequency divider with variable division ratio. Changing the distribution ratio of a frequency divider with variable division ratio on the synthesizer output we can get network frequencies with a step.

$$f_{CO} = Nf_o \tag{1}$$

$$f_o = \frac{f_{or}}{M} \tag{2}$$

where N – distribution coefficient of a frequency divider with variable division ratio;

M – distribution coefficient of a frequency divider with a fixed division factor;

f_o – the comparison frequency (a step) on the phase discriminator input.

We will carry out a spectral characteristics analysis of the selected basic structure of the voltage range exciters of the voltage inverter. For reasoning the methodology it is necessary to find the equation describing the signal spectrum at the frequency synthesizer output from its structure chart and the elements included therein [10], [11].

Pulse-phase-locked loop system can be converted on the Kotelnikov theorem basis into uninterrupted one [8], [12].

The theorem condition can be expressed in the form of inequality:

$$f_n \geq f_U \tag{3}$$

Where: f_n – the frequency of repetition;

f_U – the transmission frequency of uninterrupted particle.

It should be noted, the transition, although used in practice, but it is strict and valid only at low modulation indexes.

Following the methodology proposed in [9], [13], a generalized structure chart shown in Figure 1 can be reduced to a linear which is equivalent to the chart of the digital phase-locked loop (Figure 2).

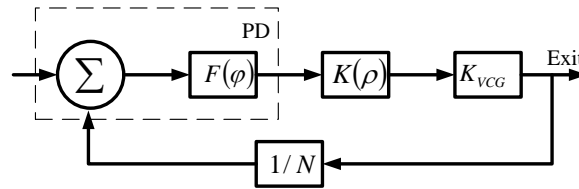The system of this type is described by the differential equation:

$$p\varphi + \frac{\Omega_y K(p) F(\varphi)}{N} = \Delta\omega_i,$$ (4)

where $K(p)$ – transfer coefficient LPF;

$\Delta\omega_i$ – the initial detuning,

Ω_y – retention strip;

$F(\varphi)$ – normalized characteristic of phase detector.

Figure 2. The equivalent circuit of digital loop PLL

The difference from a typical PLL system is the presence of feedback. From is characterized by. Here is a diagram of a standard system that will simplify the analysis.

Voltage creates at the output of the phase discriminator:

$$e_{PD} = \psi\left(U_{SG}, U_{DFVD}, \varphi^*\right),$$ (5)

where e_{PD} − voltage at the output of the phase detector which depended on amplitudes and instantaneous differences of phases of two compared oscillations U_{SG} and U_{DFVD} of a strong generator and a frequency divider with variable division ratio accordingly; φ^* − instantaneous difference of phase oscillations at the phase discriminator input.

These values are associated with the scheme parameters by following correlations:

$$U_{DFVD} = k_{DFVD} U_{VCG},$$ (6)

$$\varphi^* = \varphi_{SG} - \frac{\varphi_{VCG}}{N},$$ (7)

where U_{VCG} – voltage amplitude of a voltage-controlled generator;

k_{DFVD} – voltage transfer coefficient of DFVD;

N – distribution coefficient of DFVD;

φ_{VCG} - instantaneous phase of oscillations of VCG;

φ_{SG} – instantaneous phase of oscillations of a strong generator (SG).

To simplify the analysis we use the known ratio:

$$\Delta\omega^*(t) = 2\pi\Delta f^*(t),$$ (8)

$$\varphi^*(t) = \int \Delta\omega^*(t) dt.$$ (9)

In this expression:

$$\Delta\omega^*\left(t\right)=\frac{N\omega_{SG}-\omega_{VCG}}{N}=\frac{\Delta\omega\left(t\right)}{N}, \tag{10}$$

where $\Delta\omega^*(t)$ – instantaneous difference of frequency between VCG and some equivalent strong generator which oscillations vary with a frequency ω_{ESG} which equals to:

$$\omega_{ESG}=N\omega_{SG}. \tag{11}$$

There is a linear integral relation (8) between $\varphi^*(t)$ and $\Delta\omega^*(t)$, so we can write:

$$\varphi^*=\frac{N\varphi_{SG}=\varphi_{VCG}}{N}=\frac{\varphi}{N}, \tag{12}$$

$$\varphi=N\varphi_{SG}-\varphi_{VCG}=\varphi_{ESG}-\varphi_{VCG} \tag{13}$$

where: φ – the phase of oscillations difference between VCG and equivalent SG.

Using the correlation (5) – (12) we can form an equivalent circuit of the PLL, which considerably simplifies the analysis [14], [15]. For this we replace a real SG to an equivalent SG. VCG frequency and phase will not change their value during the transition to equivalent PD in which the amplitude is:

$$U_{VCG}^*=U_{VCG}K_{DFVD} \tag{14}$$

The output voltage of equivalent PD will be determined with the phase difference:

$$\varphi^*=\frac{\varphi}{N} \tag{15}$$

Then, considering that the DFVD effect is extended to other circuit elements (SG, VCG, PD) [16], it can be omitted. The equation for an equivalent circuit is like typical one, so:

$$p\varphi+\Omega_y F\left(\frac{\varphi}{N}\right)K_{LPF}=\Delta\omega_i. \tag{16}$$

If we talk about the complex LPF, the non-linear characteristic of PD and the control element of the equation (16) is non-linear differential equations of higher order, the exact analytical solution is associated with certain difficulties and is not currently received [16], [17].

The spectral frequency of the output signal DS is determined not only with a strong generator stable but depends on the PLL ring. PLL rings influence on the stability of the output signal DS occurs in different blocks of the random phase (frequency) modulation, due to the intrinsic noise of the circuit elements [18].

We assume that the perturbation is small and does not derive from the state of the PLL circuit matching. Then the linearization of PLL non-linear equation near steady state is easy to obtain the following linear differential equation:

$$\varphi^*+K_{LPF}\Omega_y\left|F'\left(\theta\right)\right|\varphi=\omega_{VCG}-\omega_{SG}, \tag{17}$$

where ω_{VCG} – fluctuations in the frequency of a controlled oscillator;
ω_{SG} – fluctuations in the frequency of a strong generator.

$$\theta=\arccos\left(-\frac{\Delta\omega_i}{\Omega_y}\right). \tag{18}$$

Transfer coefficient of the linear PLL has the form:

$$K(j\omega) = \frac{1}{1 + G(j\omega)}, \tag{19}$$

$$G(j\omega) = j\frac{K_{PD}S_{CE}K_{LPF}}{\omega}, \tag{20}$$

where S_{CE} – the slope of the control element VCG.

The expression for the power spectral density of the phase fluctuations VCG $S_{\varphi EXIT}$ we obtain through power spectral density of the phase fluctuations of free VCG and a strong generator, accordingly $S_{\varphi VCG}$ and $S_{\varphi SG}$:

$$S_{\varphi EXIT} = S_{\varphi VCG}\frac{1}{\left|1 + G(j\omega)\right|^2} + S_{\varphi SG}\left|\frac{G(j\omega)}{1 + G(j\omega)}\right|^2. \tag{21}$$

For further analysis, we specify the type of the phase detector. We select the type of characteristics that describes:

$$F(\theta) = \cos\theta, \tag{22}$$

$$\theta(t) = \theta_0 + \varphi(t), \tag{23}$$

where $\varphi(t)$ – small $\prec\varphi^2\succ\prec\prec 1$ random phase ratio.

As LPF we apply proportional-integrating filter, since it is common in these schemes, which transmission ratio has the form:

$$K_{LPF} = \frac{1 + j\omega T_1}{1 + j\omega T}, \tag{24}$$

where:

$$T = (R + R_1)C \tag{25}$$

$$T_1 = R_1 C_1 \tag{26}$$

Substituting (22-23) and (24) into (21) we obtain:

$$K(j\omega) = \frac{(1 + j\omega T)j\omega}{(1 + j\omega T)j\omega + \Omega_y(1 + j\omega T_1)\sin\theta}. \tag{27}$$

As it is known, the output DS wave fluctuation frequency, except for external perturbations (strong generator fluctuations) and own (fluctuations VCG) can be caused by internal noise, which together with the adjustment signal goes directly to the control element VCG. In this case, for example, for DS scheme with the converting in Figure 3, there are additional terms in the power spectral density of the phase fluctuations of the midrange output [19].

$$S_{\varphi EXIT} = S_{\varphi VCG}K_1^2(j\omega) + \left[S_{\varphi SG} + S_{\varphi DFVD} + S_{\varphi IFA} + S_{\varphi MU}\right]K_2^2(j\omega) \tag{28}$$

where:

$$K_1^2(j\omega) = \frac{\omega^2(1 + \omega^2 T^2)}{\omega^4 T^4 + \omega^2(1 + T_1\Omega_y\sin\theta_0)^2 - 2\omega^2 T\Omega_y\sin\theta_0 + (\Omega_y\sin\theta_0)^2}, \tag{29}$$

$$K_2^2(j\omega) = \frac{(\Omega\sin\theta_0)^2(1+\omega^2 T_1^2)}{\omega^4 T^2 + \omega^2(1+T_1\Omega_y\sin\theta_0)^2 - 2\omega^2 T\Omega_y\sin\theta_0 + (\Omega_y\sin\theta_0)^2}, \tag{30}$$

$S_{\varphi SG}\varphi(t)$ – the power spectral density of fluctuations in the phase of the strong generator;

$S_{\varphi VCG}$ – the power spectral density of fluctuations in the phase of VCG;

$S_{\varphi IFA}$ – the power spectral density of fluctuations in the phase of IFA;

$S_{\varphi MU}$ – the power spectral density of fluctuations in the phase of the strong generator multiplication of the frequency.
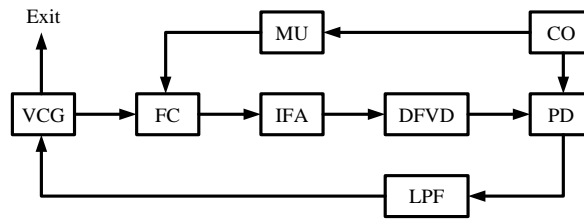
Figure 3. A structure chart of digital synthesizers
of frequencies DDS with the conversion

The expression (28) makes it possible to take into account the effect of the synthesizer circuit elements on its output.

3. Results and discussion

In order to obtain the calculated ratios we use the method of functional decomposition of Volterra and examine the equivalent model of the PLL frequency synthesizer (Figure 2) which was gotten from a structure chart of a exciter (Figure 1).

The differential equation that describes the model can be written as [10], [20]:

$$\dot{\varphi} + \Omega_y K(p) F\left(\frac{\varphi}{N}\right) = \dot{x}, \tag{31}$$

where $\dot{\varphi}$ – the difference between phases of signals of quartz and VCG generators;

Ω_y – retention strip;

$K(p)$ – transfer function of low-pass filter (LPF);

$F\left(\frac{\varphi}{N}\right) = \sin\left[\frac{\varphi}{N}\right]$ – the characteristics of the phase detector;

N – division ratio of accomplice with variable division factor (DFVD) of frequency in a synthesizer;

$\dot{x} = x(t)$ – perturbations acting on the PLL circuit due to internal noise.

Following the methodology proposed in [11], we seek a solution of the equation (31) in the form of a truncated series of Volterra:

$$\varphi(t) = \sum_{n=1}^{3} \int_{-\infty}^{+\infty} d\tau_1 \ldots \int_{-\infty}^{+\infty} d\tau_n h_n(\tau_1,\ldots,\tau_n) \prod_{i=1}^{n} x(t-\tau_i), \tag{32}$$

where - $h_n(\tau_1,\ldots,\tau_n)$ Volterra's nuclei n-th order (n= 1, 2, 3) which characterizing the PLL.

We consider the phase detector characteristic as sinusoidal and expand it in a Taylor series:

$$F\left(\frac{\varphi}{N}\right) = \sin\left(\frac{\varphi}{N}\right) = \frac{\varphi}{N} - \frac{1}{3!}\left(\frac{\varphi}{N}\right)^3 + \frac{1}{5!}\left(\frac{\varphi}{N}\right)^5 \ldots \tag{33}$$

Substituting (32) into (33) and collecting terms in order in $x(t)$ we get:

$$\left[\dot{\varphi}_1\left(t\right)+\dot{\varphi}_2\left(t\right)+\dot{\varphi}_3\left(t\right)...\right]+\frac{\Omega_y K\left(p\right)}{N}\left\{\begin{array}{l}\left[\varphi_1\left(t\right)+\varphi_2\left(t\right)+\varphi_3\left(t\right)+...\right]-\\\frac{1}{3!}\left[\varphi_1\left(t\right)+\varphi_2\left(t\right)+\varphi_3\left(t\right)+...\right]\end{array}\right\}=x\left(t\right) \quad (34)$$

Equating terms with different powers on $x(t)$ we get the following system of equations:

$$\left.\begin{array}{l}\dot{\varphi}\left(t\right)+\Omega_y K\left(p\right)^{\varphi_1\left(t\right)}\!\!\Big/\!_N=x\left(t\right)\\[2mm]\dot{\varphi}_2\left(t\right)+\Omega_y K\left(p\right)^{\varphi_2\left(t\right)}\!\!\Big/\!_N=0\\[2mm]\dot{\varphi}_3\left(t\right)+\Omega_y K\left(p\right)^{\varphi_3\left(t\right)}\!\!\Big/\!_N=\frac{\Omega_y K\left(p\right)}{3!N^3}\varphi_1^3\left(t\right)\end{array}\right\} \quad (35)$$

To find Volterra nuclei we use the theory of multidimensional transforms of Laplace. For a function of one variable a bilateral Laplace transform is given by:

$$F\left(p_1...p_n\right)=\int\limits_{-\infty}^{+\infty}dt_1...\int\limits_{-\infty}^{+\infty}dt_n f\left(t_1...t_n\right)e^{-p_1 t_1-p_2 t_2...-p_n t_n} \quad , \quad (36)$$

$$f\left(t_1...t_n\right)=\left(\frac{1}{2\pi j}\right)\int\limits_{-\infty}^{+\infty}dp_1...\int\limits_{-\infty}^{+\infty}dp_n F\left(p_1...p_n\right)e^{p_1 t_1...-p_n t_n} \quad (37)$$

Applying multidimensional Laplace transforms for both sides of equation (35), we get an expression for Volterra nuclei in the operator form:

$$H_1\left(p_1\right)=\frac{1}{p_1+\Omega_y K\left(p_1\right)\cdot\dfrac{1}{N}} \quad , \quad (38)$$

$$H_2\left(p_1,p_2\right)=0, \quad (39)$$

$$H_3\left(p_1,p_2,p_3\right)=\frac{1}{3!N^3}\cdot\frac{\Omega_y K\left(p_1+p_2+p_3\right)}{\left(p_1+p_2+p_3\right)+\Omega_y K\left(p_1+p_2+p_3\right)\cdot\!\!\!\!\!/\,_N}\cdot\prod_{i=1}^{3}\frac{1}{p_i+K\left(p_i\right)\Omega_y\cdot\!\!\!\!\!/\,_N} \quad (40)$$

Similarly, higher orders nuclei can be found. From the expressions (40) we found that the second order nucleus is 0. It can be shown that all the nuclei of paired degrees are equal to 0, in the case of odd non-linearity. Nuclei are independent of the incoming signal, they reflect the properties of the system [11], [12].

We shall restrict our analysis to the calculation of Volterra nuclei only the first three orders, because the nucleus of higher orders have little effect on the analysis results.

As the low-pass filter we use a proportional-integrating filter which have a transfer characteristic:

$$K\left(p\right)=\frac{mTp+1}{Tp+1} \quad (41)$$

where:

$$T=\left(R_1+R_2\right)C \quad (42)$$

T – filter time constant.

$$m=\frac{R_1}{R_1+R_2} \quad (43)$$

Substituting (41) into the expression for the first order nucleus (35), we get an expression for the linear approximation of phase spectrum of the rigged generator:

$$S_{\varphi_1}(\omega) = b^2\Omega_y^2 \frac{\left(T + b\Omega_y mT\right)^2 \omega^2 +}{\omega^4 + \dfrac{1}{T^2}\left[1 + 2T\Omega_y(m-1) + m^2T^2\Omega_y^2\right]\omega^2 + \dfrac{\Omega_y^2}{T^2}} \cdot \frac{+\left(a + b\Omega_y\right)^2}{\left(b\Omega_y mT\right)^2 \omega^2 + \left(b\Omega_y\right)^2} \quad (44)$$

We find an expression for the cubic approximation $f_0 = \omega/2\pi$ of the spectrum:

$$S_{\varphi_1}(p_1p_2p_3) = H_3(p_1p_2p_3)\begin{bmatrix} a^3 + 3a^2bK(p_3)\Omega_y + 3ab^2K(p_2)\cdot \\ \cdot K(p_3)\Omega_y^2 + b^3\Omega_y^3 K(p_1)K(p_2)K(p_3) \end{bmatrix}^3 \quad (45)$$

Then we draw associate variables $p_1p_2p_3$.

It is known [13] that the spectrum of the output signal $\varphi(t)$ of a non-linear dynamical system, described by a set of N Volterra nucleus in the operator form $H_n(p_1,\ldots p_n)$, can be written as:

$$\Phi(p) = \sum_{n=1}^{N} \dot{A}\left\{ H_n(p_1,\ldots,p_n)\prod_{i=1}^{n} X(p_i)\right\}, \quad (46)$$

and

$$p = j\omega \quad (47)$$

where: A − operator which leads to a single variable.

Combining (40) and (46) after the transition to the power spectral density of the phase fluctuations $S_\phi(\omega)$ we have:

$$S_\varphi(\omega) = b^2\Omega_y^2\left\{1 + \frac{1}{3!}b^2\Omega_y^3 \frac{K_1\omega^6 + K_2\omega^4 + K_3\omega^2 + K_4}{L_1\omega^8 + L_2\omega^4 + L_3\omega^2 + L_4}\right\} \cdot \frac{m^2\omega^2 + 1/T^2}{\omega^4 + \dfrac{1}{T^2}\left[1 + 2T\Omega_y(m-1) + m^2T^2\Omega_y^2\right]\omega^2 + \left(\Omega_y/T\right)^2} \quad (48)$$

where:
$b_2[1/\text{Hz}]$ – the ratio of the noise - and the signal on power in the signal band;

$$m = \frac{R_1}{R_1 + R_2} \quad (49)$$

m – proportional-integrating factor LPF;
T- time constant LPF,

$$T = (R_1 + R_2)C, \quad (50)$$

$$L_1 = B_1^2 - 2B_2, \quad L_2 = B_2^2 - 2B_1B_3 + 2B_4, \quad L_3 = B_3^3 - 2B_4B_2, \quad L_4 = B_4^2, \quad (51)$$

$$K_1 = -\left[2A_2 + A_1(2B_1 - A_1)\frac{b^2\Omega_y^3}{3!}\right], \quad (52)$$

$$K_2 = 2A_1 + 2A_2\left(2B_2 + A_2\frac{b^2\Omega_y^3}{3!}\right) + A_3\left(2B_1 - A_1\frac{b^2\Omega_y^3}{3!}\right) - A_1\left(2B_3 + A_3\frac{b^2\Omega_y^3}{3!}\right), \quad (53)$$

$$K_3 = -\left[A_4\left(2B_2 - A_2\frac{b^2\Omega_y^3}{2!}\right) + A_2\left(2B_4 + A\frac{b^2\Omega_y^3}{3!}\right) - A_3\left(2B_3 + A_3\frac{b^2\Omega_y^3}{3!}\right)\right], \quad (54)$$

$$K_4 = A_4\left[2B_4 + A_4\frac{b^2\Omega_y^3}{3!}\right], \qquad A_1 = (A+C)^3, \tag{55}$$

$$A_2 = 3A^3(B+2D) + 3A^2C(3D+4B) + 3AC^2(5B+4D) + 3C^3(2B+D), \tag{56}$$

$$A_3 = A^3(11D^2 + 4BD + 2B^2) + 9AC^2(2B^2 + 6BD + D^2) + 9AC^2(B^2 + 6BD + 2D^2) + C^3(11B^2 + 14BD + 2D^2) \tag{57}$$

$$A_4 = 3(A^3D + BC^3)(2B^2 + 5BD + 2D^2) + 27ABCD[C(2B+D) + A(2D+B)], \tag{58}$$

$$B_1 = 6\left(\frac{1}{T} + m\Omega_y\right), \qquad B_2 = 11\left(\frac{1}{T} + m\Omega_y\right)^2 + \frac{\Omega_y}{T} \tag{59}$$

$$B_3 = 6\left(\frac{1}{T} + m\Omega_y\right)^3 + 3D\frac{\Omega_y}{T}\left(\frac{1}{T} + m\Omega_y\right), \tag{60}$$

$$B_4 = 3\left(\frac{\Omega_y}{T}\right)^2 + 18\frac{\Omega_y}{T}\left(\frac{1}{T} + m\Omega_y\right) \tag{61}$$

$$A + C = m; \quad BC + AD = \frac{1}{T}; \quad B + D = \frac{1}{T} + m\Omega_y; \quad BD = \frac{\Omega_y}{T}. \tag{62}$$

As an example of the developed method, we carry out numerical calculations of the frequency stability of the range exciter.

To calculate the characteristics of stability, we substitute (32) into the expression for the relative value of the standard deviation of the СЧ output frequency from the mean value for the measurement of time [14]:

$$\frac{\sigma[\langle\varphi\rangle\tau]}{f_0} = \left(\frac{2}{\omega_0^2\tau^2}\int_0^\infty S_p(\omega)\sin\frac{\omega\tau}{2}d\omega\right)^{1/2}, \tag{63}$$

where $f_0 = \omega/2\pi$ – nominal output signal frequency of DS.

The calculation of the equations (32), (33) were carried out on the PC. The calculation results are shown in Figure 4 (the solid line). The results of calculations in the linear approximation (dashed line) are also shown here. The calculations were made for a particular frequency synthesizer with parameters $b_2 = 10^{-3}$Hz^{-1}, $\Omega_y = 40$ mHZ, $N = 20$, $m = 0.5$, $\grave{O} = 1.6 \cdot 10^{-2}$ñ, $f_0 = 1.15$ GHZ.
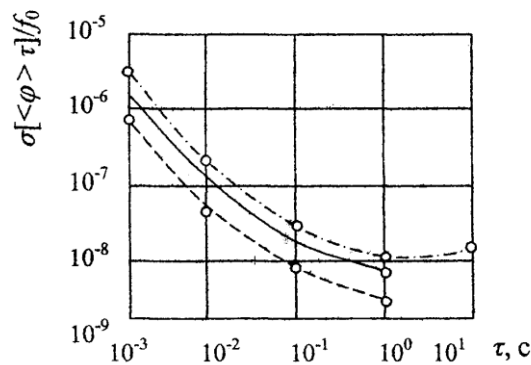
Figure 4. Characteristics of the synthesizer
frequency stability

Figure 4 also shows the experimental characteristics of the midrange frequency stability of the DS (dash-dot line). The experimental and calculated points, which conducted the curves, are marked by circles.

A comparison of these curves with the results of the linear theory shows a significant discrepancy (in order) of the obtained data. It should also be noted that the inclusion of non-linearity of the phase detector leads to a difference in the results only in quantitative terms, without changing mores of the dependence.

Thus, the above calculations of the spectral characteristics for the non-linear model of PLL indicate that the non-linearity is necessary to be taken into account only for quantitative estimates. A simple linear model of PLL can be used to analyze the process with sufficient accuracy.

4. Conclusions

The investigations have shown that the existing recommendations for the choice of parameter values of the range exciter and phase inverter synchronization systems are designed for linear models. This is the reason for the considerable discrepancy (up to 10%) between calculated and experimental values of spectral characteristics.

The analysis of the work of phase synchronization systems of load inverters, as well as the PLL based exciter, should be made taking into account the nonlinear nature of the PLL loops based on the functional method using Volterra series.

The developed calculation method allows to obtain the calculated values close enough to the experimental ones, both for the power of phase fluctuations and for the discrete components of the spectrum of the output signal. Moreover, any given accuracy can be obtained by selecting the required number of members of the series.

One main loop PLL based synthesizer with frequency divider in the feedback loop should be selected as the main structure of the voltage inverter.

References

[1]   Semenov B 2011 Power electronics: professional solutions, *Solon-Press*, Moscow, Russia

[2]   Meleshyn V 2005 Transistor converters, *Technosphere,* Moscow, Russia

[3]   Baskaran J and Pugazhendiran P 2016 Realization of Unified Power Quality Conditioner for Mitigating All Voltage Collapse Issues, *Circuits and Systems* **7**(6) 124-132

[4]   Savchenko O, Miroshnyk O, Dyubko S, Shchur T, Komada P and Mussabekov K 2019 Justification of ice melting capacity on 6-10 kV OPL distributing power networks based on fuzzy modeling, *Przegląd Elektrotechniczny* **95**(5) 106-109

[5]   Mikhalev P 2005 PLL circuits and synthesizers on the Analog Devices manufactured basis, *Components and Technology* (4) 16-21

[6]   Talbot D B 2012 *Frequency Acquisition Techniques for Phase Locked Loops*, Willey-IEEE Press, New York, USA

[7]   Pupkov K A, Kapalin V I and Yushchenko A S 2005 Functional series in the non-linear systems theory, *Nauka*, Moscow, Russia

[8]   Jovcic D 2003 Phase Locked loop system for FACTS, *IEEE Transactions on Power Systems* **18**(3) 116-1124

[9]   Ryabov I V, Tolmachev S and Strelnikov I V 2018 *Direct digital synthesizers for radio communication systems with programmable tuning of the working frequency*, 2018 Systems of Signals Generating and Processing in the Field of on Board Communications, Moscow, Russia, March 14-15, pp 17735868

[10]   Rice S O 1973 Volterra Systems With more than one input port (Distortion in a freguency conuerter), *Bell Syst Tech* 52(**8**) 1255-1270

[11]   Efkarpidis N, De Rybel T and Driesen J 2016 Technical assessment of centralized and localized voltage control strategies in low voltage networks, *Sustainable Energy, Grids and Networks*

8 85-97

[12] Van Stiphout A, Brijs T, Belmans R and Deconinck G 2017 Quantifying the importance of power system operation constraints in power system planning models: A case study for electricity storage, *Journal of Energy Storage* **13** 344-358

[13] Karlov B V 2004 Modern frequency converters: management and hardware implementation, *Power electronics* **1** 12-19

[14] Komada P, Trunova I, Miroshnyk O, Savchenko O and Shchur T 2019 The incentive scheme for maintaining or improving power supply quality, *Przegląd Elektrotechniczny* **95**(5) 79-82

[15] Panfilov D I, ElGebaly A E, Astashev M G and Rozhkov A N 2018 *New Approach for Thyristors Switched Capacitors Design for Static VAR Compensator Systems*, 2018 19th International Conference of Young Specialists on Micro/Nanotechnologies and Electron Devices (EDM), Erlagol, Russia, June 29-July 3, pp 560-566

[16] Wang H L 2015 Analysis and Applications of the Measurement Uncertainty in Electrical Testing, *Journal of Power and Energy Engineering* **3**(4) 231-239

[17] Van Roermund A, Steyaert M and Huijsing J H 2003 *Analog Circuit Design. Fractional-N Synthesizers, Design for Robustness, Line and Bus Drivers*, Kluwer Academic Publishers, Dordrecht, Netherlands

[18] Bollen M H J 2002 Definitions of Voltage Unbalance, *IEEE Power Engineering Review* **22**(11) 49-50

[19] Lysychenko R 2014 Influence investigation of the elements characteristics of range of pathogens inverter voltage converters on their spectral characteristics, *Journal of Kharkiv Petro Vasylenko National Technical University of Agriculture. Engineering, The problems of energy supply and energy efficiency and agriculture of Ukraine, KNTUA* **186** 17-19

[20] Hoornaert F, D'hulst R, Vingerhoets P, Vanthournout K and Driesen J 2016 LV distribution network voltage control mechanism: Analysis of large-scale field-test, *Sustainable Energy, Grids and Networks* **6** 7-13